

Scanning transmission low-energy electron microscopy

I. Müllerová
M. Hovorka
I. Konvalina
M. Unčovský
L. Frank

We discuss an extension to the transmission mode of the cathode-lens-equipped scanning electron microscope, enabling operation down to the lowest energies of electrons. Penetration of electrons through free-standing ultrathin films is examined along the full energy scale, and the contribution of the secondary electrons (SEs), released near the bottom surface of the sample, is shown, enhancing the apparent transmissivity of the sample to more than 100%. Provisional filtering off of the SEs, providing the dark-field signal of forward-scattered electrons, was made using an annular 3-D adjustable detector inserted below the sample. Demonstration experiments were performed on the graphene flakes and on a 3-nm-thick carbon film. Electron penetrability at the lowest energies was measured on the graphene sample.

Introduction

The transmission electron microscope (TEM) is capable of imaging individual atomic columns and, at certain conditions, even single atoms in free-standing thin foils using electrons in the energy range of hundreds of kiloelectronvolts. The scanning TEM (STEM) mode is also operated in the same energy range, mostly in the form of an attachment to a TEM device. Significant effort has been invested in achieving high resolution, even at lower energies, where we obtain lesser radiation damage and higher contrast [1]. Even sub-Ångström resolution was presented at 20 keV in an aberration-corrected TEM [2]. Recently, even low atomic number materials, such as carbon structures and biological samples or polymers, can be imaged with high contrast and lateral resolution [3–5].

Since about two decades ago, STEM attachments to the scanning electron microscopes (SEMs), which are normally used for imaging of bulk samples, started appearing more broadly [6, 7]. These are operated at energies that are usually available in the SEM, i.e., up to approximately 30 keV. Adequately thinner samples of 100 or 200 nm in thickness must be used in this case.

However, the inelastic mean-free path, which is primarily responsible for the electron penetration, starts steeply growing again below approximately 50 eV (see, e.g., [8]).

This establishes an approach to operating the STEM at tens or units of electronvolts on samples of thicknesses around or below 10 nm. More than 40 years ago, Kanter published a possibility of transmission of 1.1-eV electrons through a self-supported gold film with a thickness of 20 or 5 nm [9]. One of the first experimental setups for the measurement of transmissivity through self-supported thin films was designed by Smith and Wells [10]. In order to avoid aberrations of lenses for the long wavelength of electrons at very low energies, they used a “lensless” system in which the source of electrons (at units of electronvolts) was placed just 1 nm above the specimen and mechanically scanned across the surface while the transmitted signal was detected. Regrettably, no results obtained with this setup have been published. Thin films condensed on a metal substrate were examined using irradiation by a monoenergetic electron beam at energies below 30 eV via the signal transmitted through the surface layer into the underlying specimen and measured as the so-called absorbed current (see the overview of Sanche [11]).

We made use of the advantages of the cathode lens (CL) principle [12] to obtain high lateral resolution in the SEM down to very low energies [16]. The microscope was equipped with the detector of not only reflected electrons but also transmitted electrons (TEs). Initial results have shown the method to be a powerful tool for the examination of ultrathin films [13–15]. This paper describes imaging of 3-nm carbon foils in the reflected and transmitted mode at

Digital Object Identifier: 10.1147/JRD.2011.2156190

© Copyright 2011 by International Business Machines Corporation. Copying in printed form for private use is permitted without payment of royalty provided that (1) each reproduction is done without alteration and (2) the Journal reference and IBM copyright notice are included on the first page. The title and abstract, but no other portions, of this paper may be copied by any means or distributed royalty free without further permission by computer-based and other information-service systems. Permission to republish any other portion of this paper must be obtained from the Editor.

0018-8646/11/\$5.00 © 2011 IBM

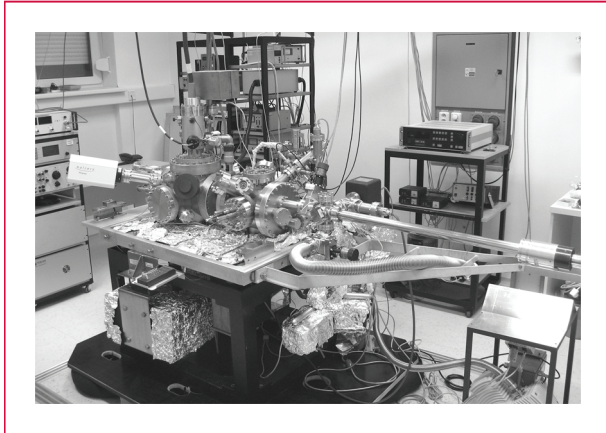


Figure 1

Ultrahigh-vacuum scanning low-energy electron microscope equipped with the cathode lens and with the detectors of reflected and transmitted electrons.

low energies and with high-resolution imaging of the graphene [16] in both signals at very low energies.

Experimental

For experiments with scanned very-low-energy electron beams, an ultrahigh-vacuum (UHV) scanning low-energy electron microscope (SLEEM) has been developed with the operational vacuum on the order of 10^{-10} mbar (see **Figure 1**). The instrument consists of three vacuum chambers, of which one is intended for observation of the specimen, the second contains facilities for *in situ* preparation procedures, and the third chamber is the loading container of the airlock. The observation chamber is equipped with a field emission gun installed into a two-lens all-electrostatic electron column with an electronically variable aperture (FEI Company). The energy range of primary electrons spans the interval from 1 to 25 keV with the ultimate resolution limit of 12 nm at 25 keV and 0.1-nA beam current. The beam current can be increased up to 100 nA.

The device has been primarily used for observation of clean or even *in situ* prepared surfaces using the image signal of very slow reflected electrons. The all-electrostatic fully bakeable electron optical column has been completed with the CL [17–19], that is, an immersion electrostatic lens in which the sample plays the role of cathode so it is biased to a high negative potential. The electrostatic field generated in this way retards the primary beam to an arbitrarily low landing energy. In this arrangement, the spot size is much less dependent on the landing energy, contrary to the conventional SEM where it enlarges proportionally to $(\text{energy})^{-3/4}$. The CL serves as an aberration corrector, reducing the spot size versus energy slope to $(\text{energy})^{-1/4}$ in a worst case, leaving it nearly energy independent under

specific conditions [17]. Thus, the CL-equipped SEM enables one to lower the landing energy without any significant loss in the image resolution. A resolution of 26 nm at 10 eV was obtained in this setup [20].

While the negatively biased specimen forms the cathode of the CL, the detector of electrons reflected to above the specimen serves as the anode on the ground potential. The detector consists of a coaxial bored single-crystal yttrium-aluminum garnet (YAG) disc of the outer/inner diameter of 10/0.3 mm, which is finely movable along all three axes. Primary beam electrons (PE) at a high energy of approximately 5 keV are retarded toward the specimen by its negative bias to their final landing energy (E_L), whereas the signal electrons are collimated and accelerated to the detector by the same field of the CL. In this way, high collection efficiency, as well as high amplification of the detector, is secured down to very low energies.

Recently, the previously described device was extended to the TE mode by introducing a TE detector to below the sample. Because the UHV operation requires the sample to be loaded through an airlock, the TE detector, based on a silicon PIN diode of size 5×5 mm (SD-61-2636), was integrated into the capsule of the airlock assembly. Signal electrons transmitted through the thin specimen are influenced by the same electrostatic field of the CL as the reflected electrons; therefore, high collection efficiency and high amplification of the TE detector are also obtainable down to the lowest energies. This simple design of the TE detector does not allow for mutual adjustment of the sample and diode, but the diode did not exhibit any important fluctuations in the local sensitivity; thus, any sample movements in the vicinity of the optical axis were not apparent in micrographs.

The basic experimental setup of the CL mode and detector assemblies is shown in **Figure 2**, together with an example of the simulated trajectories of electrons reflected or transmitted at a few specific energies.

The STEM method at very low energies has been demonstrated on a 3-nm carbon film sputtered on a gilded carbon holey foil placed on a copper grid and on the mutually overlapped graphene flakes exhibiting some spots of the single graphene shell only. Higher magnification images were taken in the Nova** NanoSEM device is equipped by the CL mode and offers operation in the energy range of 50 eV–30 keV at a high lateral resolution (3.5 nm at 100 eV and 1.4 nm at 1 keV) [21]. In an experimental setup of this microscope, we were able to operate down to landing energies very near zero.

Results and discussions

Our preliminary experience with ultrathin free-standing films has crucially shown that the conductivity of the foil is sufficient for draining the charge injected by the illuminating beam [13]. Thus, first, we successfully checked the resistance

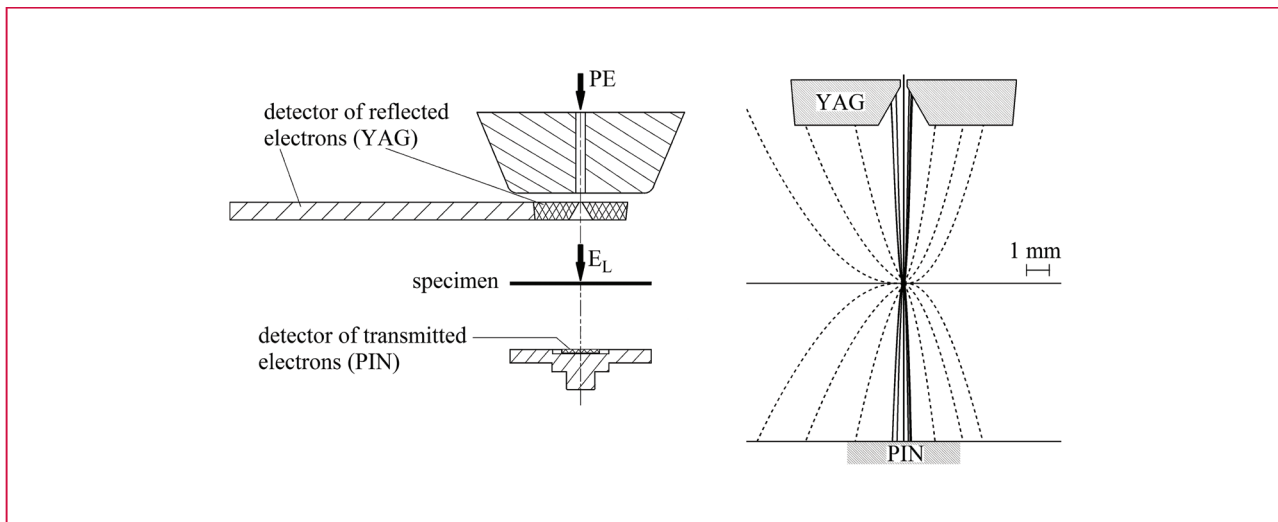


Figure 2

(Left) Cathode lens mode assembly of the UHV SLEEM, consisting of a detector of reflected electrons [YAG (yttrium–aluminum garnet) crystal] at the ground potential, a specimen on a controlled negative potential, and a focusing objective lens. PEs are decelerated by the negative potential of the specimen to the final landing energy E_L . Electrons transmitted through the specimen are collected by the detector, based on a silicon PIN diode on the ground potential. (Right) Example of the reflected and transmitted signal trajectories of electrons emitted from the specimen to the detectors. The initial energies of electrons are (solid line) 5 eV and (dashed line) 300 eV in the right half space, and (solid line) 10 eV and (dashed line) 1,000 eV for the left half space. The initial polar angles are 0° , 30° , 60° , and 90° with respect to the optical axis. The electrostatic field strength between detectors and specimen is 5 keV/7 mm.

of the carbon foil and graphene samples with respect to electron bombardment. This checking was made by acquisition of a series of micrographs throughout the full energy scale from a few kiloelectronvolts down to units of electronvolts. We did not encounter any problem with the conductivity of the specimen through the whole energy range, and the foils were also found safely adhered to the supporting grid, even when the specimen was immersed in a strong electrostatic field. We observed no influence of “microlenses” formed by the grid holes on the electron optical properties of the primary electron beam, in the final image.

Figure 3 shows micrographs of the 3-nm carbon foil on a gilded carbon hole-filled foil placed on a Cu grid, which was obtained when acquiring the backscattered electrons (BSEs) and the TEs at “medium” landing energies. At 3 keV, the carbon film is fully transparent, and even some signal passes the supporting foil. At 98 eV, we still obtain some transmissivity of the 3-nm carbon film. The BSE image enables us to distinguish between the sites covered by the film and the empty holes. Thus, we are able to reveal a peculiar phenomenon consisting of empty holes in the sample, which are darker than the neighboring layer. This would indicate the electron transmissivity of the film exceeding 100%. The effect appeared in the range of hundreds of electronvolts and was observed to be repeating itself systematically with all specimens under examination.

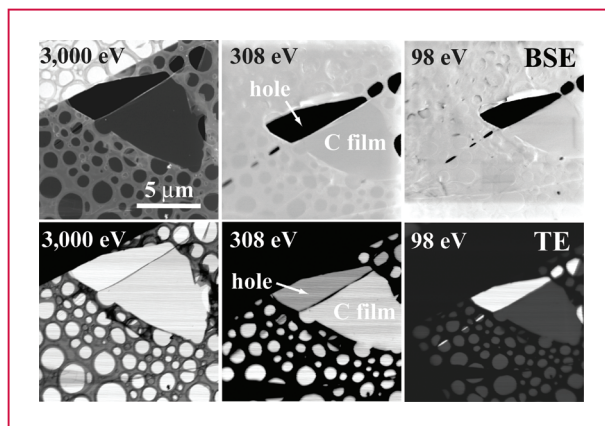


Figure 3

Three-nanometer-thick carbon film on a gilded carbon hole-filled foil, placed on a Cu grid (sample provided by the University of Zurich). The primary beam energy was 6 keV; the landing energies (starting from the left) are 3,000, 308, and 98 eV. Micrographs are taken in the (upper row) reflected and (lower row) transmitted electrons. The experiment was conducted in UHV SLEEM.

In the middle column of Figure 3, we see the effect at 308 eV, where there is a large hole that is partially covered by the carbon film. As can be seen in the BSE images, the upper part of the hole is not covered by carbon (dark), but the lower

part is (bright). However, in the TE image (308 eV), the holes appear darker than the carbon-covered regions.

An explanation involves the unscattered and forward-scattered electron signal, that is, the signal of the TEs from the illumination beam, which is significantly contributed by “incoherent” secondary electrons (SEs) released near the bottom surface of the sample. The detected yield of SE increases at low energies and exhibits its maximum just in the range of hundreds of electronvolts, similarly as it does with the SEs emitted to above the upper surface of a bulk specimen. The SE emitted from the bottom surface is released by both primary and scattered electrons penetrating to the near-surface layer through the rest of the specimen. These exciting species must have much broader energy and angular distributions than the primary electrons alone, which bombard the SE emitting layer near the upper surface. However, the SE emitted in the reflection mode from bulk specimens also contains SEII released by BSE upon their return toward the surface. When the energy of electrons decreases, one would expect in the emission from the bottom surface a higher proportion of SEII, which is released with primary electrons that had survived some scattering events. This is due to the progressively shortening mean-free path and the increasing rate of the elastic scattering that broadens the bundle of electrons penetrating the layer. Consequently, the signal from the bottom surface can be expected to be less defined and hence less capable of bearing any useful information, except a possible thickness contrast. This is why we call this signal contribution “incoherent” and consider it undesirable. Obviously, one has to be very careful with interpretation of the TE flux measured behind thin samples at medium and low energies.

Let us note that, although SEs are similarly generated in any STEM device, in the absence of a field between the sample and the detector, they are too slow to be detected. In our case, SEs are accelerated toward the TE detector to energy sufficient for the generation of the signal. However, at landing energies in and above the range of tens of electronvolts, the SEs are collimated near the optical axis, leaving the elastically scattered electrons concentrated in a broader bundle. This difference in trajectories, playing the role of energy dispersion, suggests that energy filtering to remove the SE signal is possible.

In order to suppress the SE contribution to the signal, an upgraded version of the TE detector was introduced. The TE detector was split into two concentric channels, similar to the way the bright-field and dark-field channels are arranged in a conventional STEM. This design enabled us to direct SE completely to the central channel (naturally together with a part of unscattered electrons of the bright-field signal), whereas the annular channel acquires the forward scattered electrons as the dark-field signal (see the simulated electron trajectories in Figure 2). The upgraded version of the TE detector with the PIN diode,

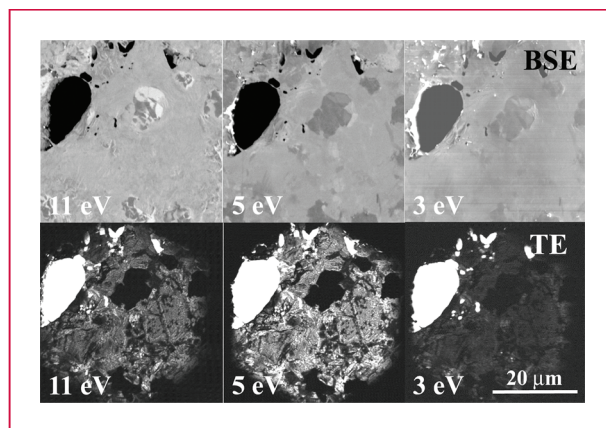


Figure 4

Graphene deposited on a supporting grid, shown in the reflected mode (BSE, upper row) and in the transmitted signal (TE, lower row). The primary beam energy was 6 keV; the landing energies (starting from the left) are 11, 5, and 3 eV. The specimen was provided by Geim from the University of Manchester as part of the EU STREP Project 028326. The experiment was conducted in the UHV SLEEM.

which is already fully adjustable in all three directions, is inserted inside the sample capsule through a side opening. The proper diode has its central circular part of 1 mm in diameter etched off; thus, it is made “blind,” leaving undamaged correct functioning around the spot. Thus, we obtain functionless the central “bright-field channel,” but the retractable mechanism enables one to center the diode to the optical axis and to detect the sole dark-field signal free of SEs or to shift it off the axis and collect the complete transmitted signal, at least at tens and units of electronvolts [22].

Figure 4 shows a series of micrographs of the mutually overlapped graphene flakes, which were taken at very low energies. The reflected signal images serve to identify holes in the graphene.

An interesting property of a filmlike graphene is its transmissivity for electrons at various energies. These data may be important in applications utilizing the film as a support, e.g., for the point-projection electron microscopy at low energies [23, 24]. The transmissivity was measured below 30 eV in the total transmitted flux mode in several spots on the sample where only a single graphene shell could be expected. We found a transmissivity minimum at 10 eV and maximum at 5 eV, and then, the transmitted flux decreases toward 1 eV. Obviously, electron energy close to 5 eV (see Figure 4) is optimal when using the graphene as a transparent support for any electron microscopic or spectroscopic mode. However, anisotropy of slow-electron passage through graphene [25] has to be taken into account.

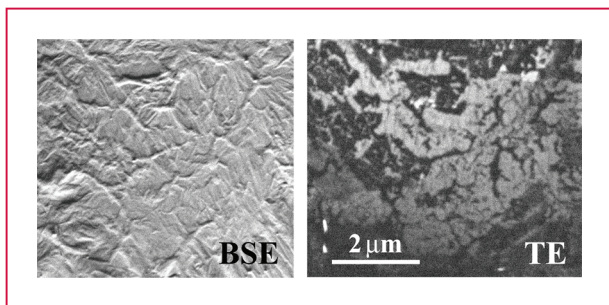


Figure 5

Higher magnification micrographs of the structure shown in Figure 4, imaged in an experimental setup of the Nova NanoSEM at the FEI Company, Brno, Czech Republic. The electrostatic field strength of the CL is 5 kV/5 mm, and the landing energy is 20 eV.

The graphene flakes were observed not only under UHV conditions; similar results were obtained under standard vacuum conditions in the commercially available SEM Nova NanoSEM. In this microscope, much better lateral resolution can be obtained than in the experimental UHV SLEEM previously described. Micrographs of the graphene flakes at a higher magnification are shown in **Figure 5** in BSEs and TEs at the landing energy of 20 eV. The BSEs obviously offer the topographical contrast only, whereas the TEs exhibit essentially four grayscale levels, which may hypothetically be identified with the number of graphene shells locally overlapped.

Conclusion

The standard SEM and the low-energy electron microscope have been used to examine surface structures using reflected electrons. The CL principle with a negatively biased sample, which was used in emission microscopes, has been introduced in the SEM in order to work at an arbitrarily low energy. The anode of the CL, which was inserted above the sample, consists of a one-channel scintillation detector with a small central bore (0.3 mm) and collects reflected electrons accelerated in the CL field and collimated toward the optical axis. Another detector, based on the PIN structure, has been positioned below the sample and has acquired the signal transmitted through thin foils and similarly accelerated and collimated. In the very low energy range, we have relied on the inelastic mean-free path of electrons steeply extending below approximately 50 eV and, hence, on increased penetrability of electrons, at least through crystalline layers. The demonstration experiments have been conducted on the sample of overlapped graphene layers with some single-layer islands deposited on a supporting grid. Micrographs in the total transmitted signal at very low energies exhibit a very high thickness contrast, obviously sensitive to individual atomic layers. The energy dependence of the transmitted

signal from the single-layer islands achieves the maximum transmissivity at 5 eV.

The reflected electron micrographs are useful for navigation and to enable one to distinguish the thinnest areas from empty holes. Similar results have been obtained with a 3-nm foil of gold [13]. The maximum transmissivity (even higher than 100%) has been measured for multiple samples at landing energies around 300 eV. This effect has been explained on the basis of the SE emission released with primary and forward-scattered electrons penetrating sufficiently near the exit surface of the foil. Experiments have been performed in the experimental UHV SLEEM, and micrographs at higher magnification have been taken in the Nova NanoSEM.

Acknowledgments

The work is supported in part by the Grant Agency of the Academy of Sciences of the Czech Republic under Project IAA100650902 and in part by the European Commission and Ministry of Education, Youth, and Sports of the Czech Republic (EC and MEYS CR) under Project CZ.1.05/2.1.00/01.0017.

**Trademark, service mark, or registered trademark of FEI Company in the United States, other countries, or both.

References

1. A. DeLong, K. Hladil, and V. Kolařík, "A low-voltage transmission electron microscope," *Eur. Microscopy Anal.*, pp. 13–15, Jan. 1994.
2. U. Kaiser, J. Meyer, J. Biskupek, J. Leschner, L. Lechner, S. Kurasch, Z. Lee, A. N. Khlobystov, H. Müller, P. Hartel, M. Haider, S. Eychus, G. Benner, and H. Rose, "Towards sub Ångström low voltage electron microscopy (SALVE); first results of Cs corrected transmission electron microscopy at 20 kV," in *Proc. 17th Int. Microsc. Congr.*, 2010, [CD-ROM].
3. O. L. Krivanek, M. F. Chisholm, V. Nicolosi, T. J. Pennycook, G. J. Corbin, N. Dellby, M. F. Murfitt, C. S. Own, Z. S. Szilagy, M. P. Oxley, S. T. Pantelides, and S. J. Pennycook, "Atom-by-atom structural and chemical analysis by annular dark-field electron microscopy," *Nature*, vol. 464, no. 7288, pp. 571–574, Mar. 2010.
4. L. F. Drummy, J. Yang, and D. C. Martin, "Low-voltage electron microscopy of polymer and organic molecular thin films," *Ultramicroscopy*, vol. 99, no. 4, pp. 247–256, Jun. 2004.
5. F. Lednický, E. Coufalová, J. Hromádková, A. DeLong, and V. Kolařík, "Low-voltage TEM imaging of polymer blends," *Polymer*, vol. 41, no. 13, pp. 4909–4914, Jun. 2000.
6. V. Morandi and P. G. Merli, "Contrast and resolution versus specimen thickness in low energy scanning transmission electron microscopy," *J. Appl. Phys.*, vol. 101, no. 1, pp. 114917-1–114917-8, Jun. 2007.
7. P. G. Merli, V. Morandi, and F. Corticelli, "Backscattered elektron imaging and scanning transmission elektron microscopy imaging of multi-layers," *Ultramicroscopy*, vol. 94, no. 2, pp. 89–98, Feb./Mar. 2003.
8. H.-J. Fitting, E. Schreiber, and K. A. von Czarnowski, "Attenuation and escape depths of low-energy electron emission," *J. Electron Spectrosc. Rel. Phenom.*, vol. 119, no. 1, pp. 35–47, Jul. 2001.
9. H. Kanter, "Slow-electron beam attenuation by gold films," *Appl. Phys. Lett.*, vol. 10, no. 3, pp. 73–75, Feb. 1967.

10. D. A. Smith and O. C. Wells, "Low-energy scanning transmission electron microscope," U.S. Patent 4 618 767, 1986.
11. L. Sanche, "Interactions of low-energy electrons with atomic and molecular solids," *Scanning Microsc.*, vol. 9, no. 3, pp. 619–656, 1995.
12. A. Recknagel, "Theorie des elektrischen Elektronenmikroskops für Selbststrahler," *Z. Phys.*, vol. 117, no. 11/12, pp. 689–708, Aug. 1941.
13. I. Müllerová, M. Hovorka, J. Sobota, R. Hanzlíková, T. Fořt, and L. Frank, "Transmission through thin films by low energy scanning electron microscopy," in *Proc. MC*, vol. 1, G. Kothleitner and M. Leisch, Eds., Graz, Austria, 2009, vol. 1, pp. 163–164.
14. I. Müllerová, M. Hovorka, and L. Frank, "Advances in low energy scanning electron microscopy," in *Proc. 17th Int. Microsc. Conf.*, Rio de Janeiro, Brazil, 2010, pp. 256–257.
15. I. Müllerová, M. Hovorka, R. Hanzlíková, and L. Frank, "Very low energy scanning microscopy of free-standing ultrathin films," *Mater. Trans.*, vol. 51, no. 2, pp. 265–270, 2010.
16. P. Blake, E. W. Hill, A. H. Castro Neto, K. S. Novoselov, D. Jiang, R. Yang, T. J. Booth, and A. K. Geim, "Making graphene visible," *Appl. Phys. Lett.*, vol. 91, no. 6, pp. 063124-1–063124-3, Aug. 2007.
17. I. Müllerová and L. Frank, "Scanning low-energy electron microscopy," *Adv. Imag. Electron Phys.*, vol. 128, pp. 309–443, 2003.
18. I. Müllerová and L. Frank, "Very low energy microscopy in commercial SEMs," *Scanning*, vol. 15, no. 4, pp. 193–201, 1993.
19. L. Frank and I. Müllerová, "Strategies for low- and very-low-energy SEM," *J. Electron Microsc.*, vol. 48, no. 3, pp. 205–219, 1999.
20. I. Müllerová and L. Frank, "Ultrahigh vacuum scanning low energy electron microscope (UHV SLEEM) for surface studies," in *Proc. 2nd Annu. Meeting Czechoslovak Microsc. Soc.*, L. Frank, Ed., 2002, pp. 79–82.
21. FEI Company, *Nova NanoSEM Scanning Electron Microscope*. [Online]. Available: <http://www.fei.com/products/scanning-electron-microscopes/nova.aspx>
22. I. Müllerová, M. Hovorka, and L. Frank, "Examination of very thin free-standing films with slow electrons," in *Proc. JCNCs*, Toyama, Japan, 2010, pp. 1–4.
23. H.-W. Fink and H. Schmid, "Atomic resolution in lensless low-energy electron holography," *Phys. Rev. Lett.*, vol. 67, no. 12, pp. 1543–1546, Sep. 1991.
24. H.-W. Fink, H. Schmid, E. Ermantraut, and T. Schulz, "Electron holography of individual DNA molecules," *J. Opt. Soc. Amer. A, Opt. Image Sci. Vis.*, vol. 14, no. 9, pp. 2168–2172, Sep. 1997.
25. R. M. Tromp, "Low energy electron microscopy: A 10 year outlook," in *Proc. 14th Eur. Microsc. Congr.*, vol. 1, M. Luysberg, K. Tillmann, and T. Weirich, Eds., Aachen, Germany, 2008, vol. 1, pp. 735–736.

Received October 11, 2010; accepted for publication
February 14, 2011

Ilona Müllerová *Institute of Scientific Instruments ASCR, v.v.i., Královopolská 147, 612 64 Brno, Czech Republic (ilona@isibrno.cz).*

Miloš Hovorka *Institute of Scientific Instruments ASCR, v.v.i., Královopolská 147, 612 64 Brno, Czech Republic (hovorka@isibrno.cz).*

Ivo Konvalina *Institute of Scientific Instruments ASCR, v.v.i., Královopolská 147, 612 64 Brno, Czech Republic (kimiki@isibrno.cz).*

Marek Unčovský *FEI Czech Republic s.r.o., Podnikatelská 6, 61200 Brno, Czech Republic, (Marek.Uncovsky@fei.com).*

Luděk Frank *Institute of Scientific Instruments ASCR, v.v.i., Královopolská 147, 612 64 Brno, Czech Republic (ludek@isibrno.cz).*